

## SEARCH FOR SIGNATURES OF PHASE TRANSITION AND CRITICAL POINT IN HEAVY-ION COLLISIONS

*M. V. Tokarev*<sup>a, 1</sup>, *I. Zborovský*<sup>b, 2</sup>, *A. Kechechyan*<sup>a</sup>, *A. Alakhverdyants*<sup>a</sup>

<sup>a</sup> Joint Institute for Nuclear Research, Dubna

<sup>b</sup> Nuclear Physics Institute, Academy of Sciences of the Czech Republic, Řež, Czech Republic

The general concepts in the critical phenomena related with the notions of «scaling» and «universality» are considered. Behavior of various systems near a phase transition is displayed. Search for clear signatures of the phase transition of the nuclear matter and location of the critical point in heavy-ion collisions (HIC) is discussed. The experimental data on inclusive spectra measured in HIC at RHIC and SPS over a wide range of energies  $s_{NN}^{1/2} = 9\text{--}200$  GeV are analyzed in the framework of  $z$ -scaling. A microscopic scenario of the constituent interactions is presented. Dependence of the energy loss on the momentum of the produced hadron, energy and centrality of the collision is studied. Self-similarity of the constituent interactions described in terms of momentum fractions is used to characterize the nuclear medium by «specific heat» and colliding nuclei by fractal dimensions. Preferable kinematical regions to search for signatures of the phase transition of the nuclear matter produced in HIC are discussed. Discontinuity of the «specific heat» is assumed to be a signature of the phase transition and the critical point.

Рассматриваются общие свойства критических явлений, связанные с понятиями «скейлинг» и «универсальность». Представлены иллюстрации поведения различных систем вблизи фазового перехода. Обсуждается поиск «чистых» сигнатур фазового перехода в ядерной материи и положения критической точки в столкновениях тяжелых ионов. Представлены результаты анализа в рамках теории  $z$ -скейлинга экспериментальных данных по инклюзивным спектрам частиц, измеренным в столкновениях тяжелых ионов на RHIC и SPS в области энергий  $s_{NN}^{1/2} = 9\text{--}200$  ГэВ. Обсуждается микроскопический сценарий взаимодействия конститuentов. Изучены зависимости потерь энергии конститuenta от импульса регистрируемой частицы, энергии и центральности столкновения. Свойство самоподобия взаимодействия, описываемое в терминах долей импульсов сталкивающихся ядер, используется для характеристики ядерной среды с помощью удельной теплоемкости ( $c$ ) и фрактальной размерности ( $\delta, \varepsilon$ ). Обсуждается кинематическая область при столкновении ядер, наиболее предпочтительная для поиска сигнатур фазового перехода в ядерной материи и критической точки. В качестве такой сигнатуры в работе предлагается скачок «удельной теплоемкости».

PACS: 25.75.-q; 25.75.Bh; 25.75.Nq; 24.80.+y

---

<sup>1</sup>E-mail: tokarev@jinr.ru

<sup>2</sup>E-mail: zborovsky@ujf.cas.cz

## INTRODUCTION

Search for clear signatures of the phase transition and location of the critical point in heavy-ion collisions is the main goal of the Beam Energy Scan Programs at SPS and RHIC [1, 2]. The programs are aimed at gaining a better understanding of the properties of the nuclear matter produced in the interactions of heavy nuclei. The existing experimental data have already revealed a striking similarity in the behavior of the inclusive spectra at the energies where the measurements have been performed till now. This is traditionally related with the ideas of self-similarity of hadron interactions which is a very fruitful concept to study collective phenomena in the hadron and nuclear matter [3, 4]. Important manifestation of this concept is a notation of scaling itself. Scaling in general means self-similarity at different scales. The physical content meant by it can be of a different origin. Some of the scaling features constitute pillars of modern critical phenomena. A brief overview of the examples associated with the existence of phase transitions in solids, liquids, and gases is given in Sec. 1. Another category of scaling laws reflects the features not related to the phase transitions (self-similarity in point explosion, laminar fluid flow, etc.). Properties of  $z$ -scaling (see [5–10] and references therein), which in a sense pertains to the both mentioned groups, are discussed in Sec. 2. It is treated as manifestation of the self-similarity property of the structure of colliding objects (hadrons, nuclei), the interaction mechanism of their constituents, and the process of constituent fragmentation into real hadrons. Features of  $z$ -scaling in  $pp$  and  $AA$  collisions are presented in Secs. 3 and 4. The validity of  $z$ -scaling is confirmed in the region which is far from the boundary of the phase transition or the region where the Critical Point (CP) can be located. Nevertheless, the  $z$ -scaling approach can be a suitable tool to search for the phase transitions and the critical point in the hadron and nuclear matter as well. The parameters of  $z$ -scaling  $c$ ,  $\delta$ , and  $\varepsilon_F$  have a physical interpretation of the heat capacity of the produced matter, a fractal dimension of the structure of hadrons or nuclei, and a fractal dimension of the fragmentation process, respectively. Although  $z$ -scaling gives us no direct information on existence of the phase transition or the critical point, change of its parameters could indicate the vicinity of the critical phenomena. The possibilities of using  $z$ -scaling for this type of investigations are discussed in Sec. 5.

### 1. SCALING & PHASE TRANSITION

This section is devoted to the consideration of self-similarity of various systems near the phase transition. The concepts developed to understand the critical phenomena are «scaling» and «universality». Scaling means that the system near the critical point exhibiting self-similar properties is invariant under transformation of the scale. According to universality, quite different systems behave in a remarkably similar way near the respective critical point [11].

The scaling theory was first introduced by B. Widom [12] to describe the behavior of simple fluids near critical points, and later extended to describe the scaling equation of the state of liquid–gas and other systems including ferromagnetic, order-disorder alloys, ferroelectrics, superconductors, as well as the systems exhibiting superfluidity. Later the scaling hypothesis was independently developed by several scientists, including Widom, Domb and Hunter,

Kadanoff, Patashinskii and Pokrovskii, and Fisher (see [13–24] and references therein). The scaling hypothesis has two categories of predictions, both of which have been remarkably well verified by the wealth of experimental data in diverse situations. The first category is a set of equations, called scaling laws (Widom, Rushbrooke, Fisher, Griffiths, Josephson, Coopersmith), that serve to relate various critical-point exponents ( $\alpha$ ,  $\beta$ ,  $\gamma$ ,  $\delta$ ,  $\nu$ ,  $\eta$ ,  $\phi$ ,  $\zeta$ ) [12, 25–30]. The scaling theory based on the assumption that the singular part of the particular thermodynamic potential is asymptotically a generalized homogeneous function (GHF) if the system is close enough to the critical point. It also means that all derivatives of the potential near CP are generalized homogeneous functions (heat capacity, compressibility, susceptibility, etc.). The second category of predictions is a sort of data collapse. It means that data can be «collapsed» onto a single curve.

A classical example of this is the Guggenheim plot shown in Fig. 1 — the temperature dependence of the scaled density  $\rho/\rho_c = (\rho_L + \rho_G)/2\rho_c \sim |T/T_c|^\beta$  for different fluids (Ne, Ar, Kr, Xe, N<sub>2</sub>, O<sub>2</sub>, CO, CH<sub>4</sub>). The critical exponent  $\beta$  was found to be equal to  $\approx 1/3$ . As is seen from Fig. 1, the data «collapse» onto a single curve according to the law of the corresponding state over a wide range of ratios  $0 < \rho/\rho_c < 2.5$  and  $0.55 < T/T_c < 1$ .

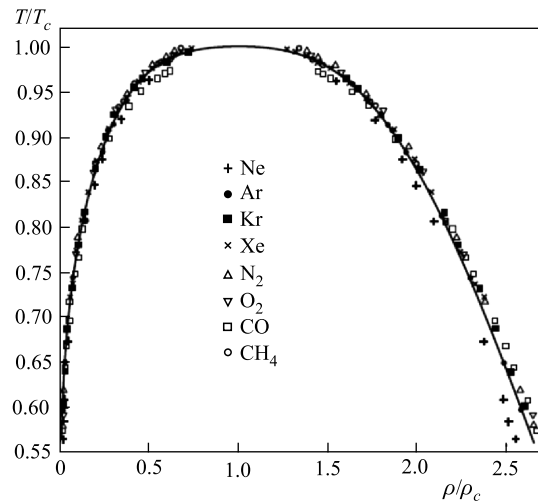


Fig. 1. The coexistence curve (the scaled density  $\rho/\rho_c$  vs. the scaled temperature  $T/T_c$ ) for different fluids [30]. The solid curve is fitted with the cubic equation  $\rho/\rho_c \sim |T/T_c|^{1/3}$

The universality hypothesis reduces the great variety of critical phenomena to a small number of equivalence classes, the so-called universality classes [14], which depend only on few fundamental parameters. All the systems belonging to the given universality class have the same critical exponents and the corresponding scaling functions become identical near the critical point. The universality has its origin in the long-range character of the fluctuations. Close to the transition point, the behavior of the cooperative phenomena becomes independent of the microscopic details of the considered system. For the short-range interacting equilibrium systems, the fundamental parameters determining the universality class are the symmetry of the order parameter and the dimensionality of space. The concept of universality remains the

major tool to study the great variety of non-equilibrium phase transitions as well (see [31] and references therein). It is known that the scaling functions vary more widely between different universality classes than the exponents. Thus, universal scaling functions offer a sensitive and accurate test for the system universality class. The universal scaling functions have also demonstrated the robustness of the given universality class.

The dependence of drag coefficient  $\zeta$  on Reynolds number  $Re$  for a circular sphere by the uniform flow is shown in Fig. 2, *a* [32]. Both the laminar flow and the turbulent one are described by the universal dimensionless function. Discontinuity of  $\zeta = \zeta(Re)$  near the point  $Re \approx 3 \cdot 10^6$  indicates the phase transition from the laminar flow to the turbulent one.

Some regimes of water flows around the cylinder at different  $Re$  are shown in Figs. 2, *b, c, d*. This example confirms that the self-similarity is common for the both types of the flows.

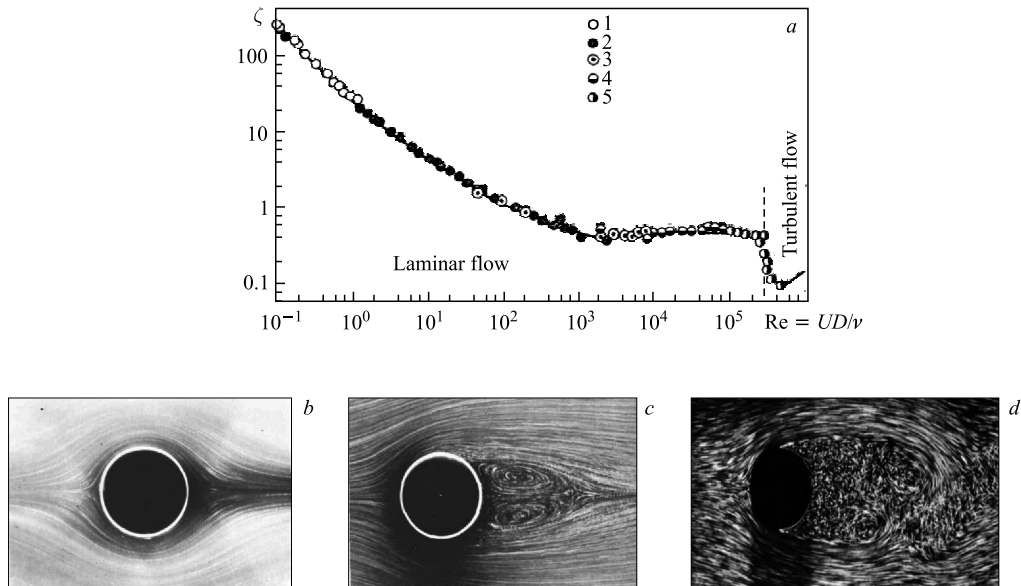


Fig. 2. *a*) Variation of the drag coefficient  $\zeta$  with Reynolds number  $Re$  for sphere [32]. Points are the experimental data. The uniform flow passes over the circular cylinder at  $Re = 0.16$  (*b*),  $Re = 26$  (*c*), and  $Re = 2000$  (*d*) [33]

As an example of the critical behavior of the system we have shown the anomaly in the temperature dependence of the specific heat  $c \sim |T - T_\lambda|^{-\alpha}$  under saturated vapor pressure for  ${}^4\text{He}$  close to the « $\lambda$ -point» [10] in Fig. 3. The temperature scales are expanded by a factor of  $10^3$ . The critical-point exponent  $\alpha$  is extremely small and therefore the divergence of the specific heat corresponds to the logarithmic law. Discontinuity of the specific heat is clearly seen at highest temperature resolution.

Impurities and defects exert strong influence upon the phase transition and physical properties of systems (for example, crystals, liquids, etc.). So, the possibilities of crystal properties modification due to directed implantation of impurities or ionizing irradiation influence of

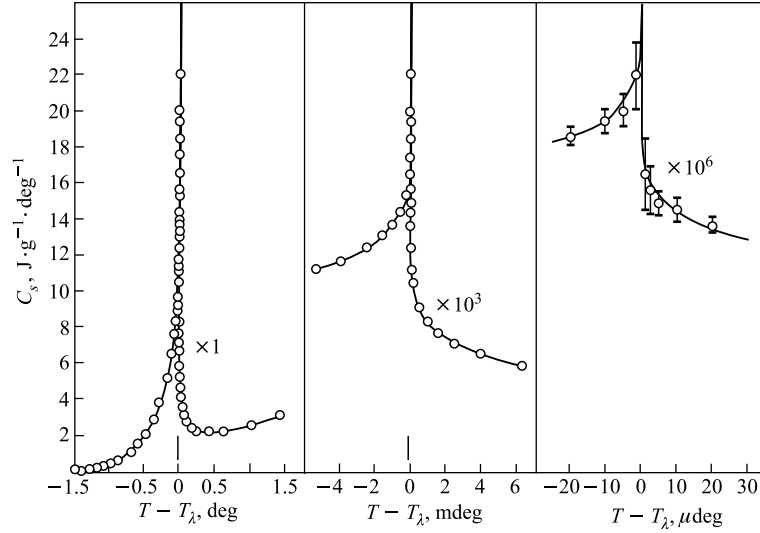


Fig. 3. Specific heat of  ${}^4\text{He}$  as a function of  $T - T_\lambda$  [11]

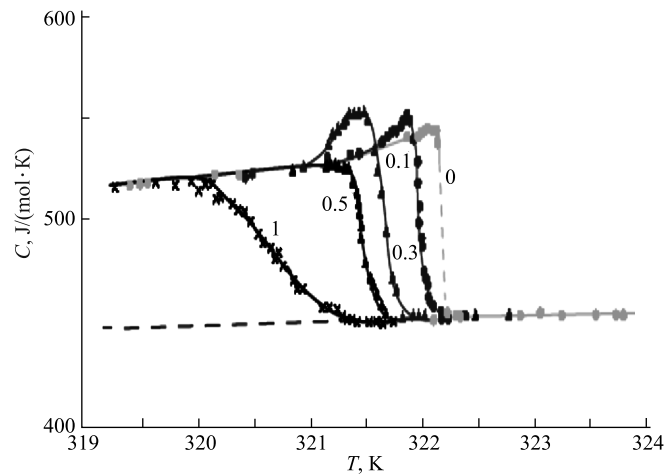


Fig. 4. Specific heat of ferroelectric crystal  $(\text{CH}_2\text{NH}_2\text{COOH})_3\text{H}_2\text{SO}_4$  undergoing radiation as a function of the temperature [34]. The dose of irradiation is shown in megaröntgens

defects on the anomalies of the crystal properties in the region of the phase transitions and on the domain structure of ferroelectric crystals are widely studied [34].

Figure 4 shows the temperature dependence of the specific heat of the ferroelectric crystal  $(\text{CH}_2\text{NH}_2\text{COOH})_3\text{H}_2\text{SO}_4$  undergoing  $\gamma$  radiation. The dramatic ionizing irradiation influence upon phase transitions is seen in Fig. 4. It results in superfluous thermal capacity and decreasing the critical temperature well determined at a low dose (0.1–0.5 MR) and smearing the temperature dependence of the specific heat at a large irradiation dose (1 MR). The observed features, as well as the other ones (dielectric susceptibility, pyroelectric coefficients, piezoelectric modules, etc.), are related to structural modification of a crystal [34].

## 2. $z$ -SCALING

The  $z$ -scaling belongs to the scaling laws with applications not limited to the regions near the phase transition. The scaling regularity concerns hadron production in the high-energy proton (antiproton) and nucleus collisions [5–10]. It manifests itself in the fact that the inclusive spectra of various types of particles are described with the universal scaling function. The function  $\Psi(z)$  depends on single variable  $z$  in a wide range of the transverse momentum, registration angles, collision energies, and centralities. The scaling variable is expressed by the formula

$$z = z_0 \Omega^{-1}. \quad (1)$$

Here  $z_0$  and  $\Omega$  are functions of kinematic variables:

$$z_0 = \frac{\sqrt{s_{\perp}}}{(dN_{\text{ch}}/d\eta|_0)^c m_N}, \quad (2)$$

$$\Omega = (1 - x_1)^{\delta_1} (1 - x_2)^{\delta_2} (1 - y_a)^{\varepsilon_F} (1 - y_b)^{\varepsilon_F}. \quad (3)$$

The quantity  $z_0$  is proportional to the transverse kinetic energy of the selected binary constituent subprocess required for the production of inclusive particle  $m$  and its partner (antiparticle). The multiplicity density  $dN_{\text{ch}}/d\eta|_0$  of charged particles in the central region  $\eta = 0$ , the nucleon mass  $m_N$ , and parameter  $c$  completely determine the functional relationship of the dimensionless variable  $z_0$ . The parameter  $c$  has the meaning of «specific heat capacity» of the medium produced in the collisions.

The quantity  $\Omega$  is proportional to a relative number of the configurations at the constituent level which include the binary subprocesses corresponding to the momentum fractions  $x_1$  and  $x_2$  of colliding hadrons (nuclei) and to the momentum fractions  $y_a$  and  $y_b$  of the secondary objects just produced in these subprocesses. The parameters  $\delta_1$  and  $\delta_2$  are fractal dimensions of the colliding objects, and  $\varepsilon_F$  stands for the fractal dimension of the fragmentation process. The selected binary subprocess, which results in production of the inclusive particle and its recoil partner (antiparticle), is defined by the maximum of  $\Omega(x_1, x_2, y_a, y_b)$  with the kinematic constraint

$$\left( x_1 P_1 + x_2 P_2 - \frac{p}{y_a} \right)^2 = M_X^2. \quad (4)$$

Here  $M_X = x_1 M_1 + x_2 M_2 + m/y_b$  is the mass of the recoil system in the subprocess. The 4-momenta of the colliding objects and the inclusive particle are  $P_1, P_2$ , and  $p$ , respectively. Equation (4) accounts for the locality of the interaction at the constituent level and sets a restriction on the momentum fractions  $x_1, x_2, y_a, y_b$  of particles via the kinematics of the constituent interactions. A microscopic scenario of constituent interactions is based on dependences of the momentum fractions on the collision energy, transverse momentum, and centrality.

The scaling variable  $z$  has a property of the fractal measure, it grows in the power manner with the increasing resolution  $\Omega^{-1}$  with respect to the constituent subprocesses. The scaling function  $\Psi(z)$  is expressed in terms of the experimentally measurable quantities — the inclusive cross section  $E d^3\sigma/dp^3$ , the multiplicity density  $dN/d\eta$ , and the total inelastic cross section  $\sigma_{\text{in}}$  — for the inclusive reaction  $P_1 + P_2 \rightarrow p + X$ . It is determined by the following expression:

$$\Psi(z) = \frac{\pi}{(dN/d\eta)\sigma_{\text{in}}} J^{-1} E \frac{d^3\sigma}{dp^3}. \quad (5)$$

Here  $J$  is Jacobian for the transition from the variables  $\{p_T, y\}$  to  $\{z, \eta\}$ . The function  $\Psi(z)$  satisfies the normalization condition

$$\int_0^{\infty} \Psi(z) dz = 1. \quad (6)$$

Equation (6) allows us to interpret  $\Psi(z)$  as probability density of the production of the inclusive particle with the corresponding value of variable  $z$ .

### 3. SCALING IN $pp$ COLLISIONS

The self-similarity properties of the particle production in proton–proton collisions provide the basis for analyzing proton–nucleus and nucleus–nucleus interactions, and verifications of the theory. Figure 5 shows spectra of the hadrons produced in proton–proton interactions in  $z$  presentation. The kinematic region covers a wide range of the collision energies, registration angles, and transverse momenta. The scale factors are introduced to split the data into different groups. The solid line is a fitting curve for these data. The derived representation shows the universality of the shape of the scaling curve  $\Psi(z)$  for different types of hadrons. The found regularity (the shape of the function  $\Psi(z)$  and its scaling behavior in the wide kinematic range at constant values of the parameters  $\delta, \varepsilon_F$ , and  $c$ ) is treated as manifestation of the self-similarity of the structure of colliding objects, interaction mechanism of their constituents,

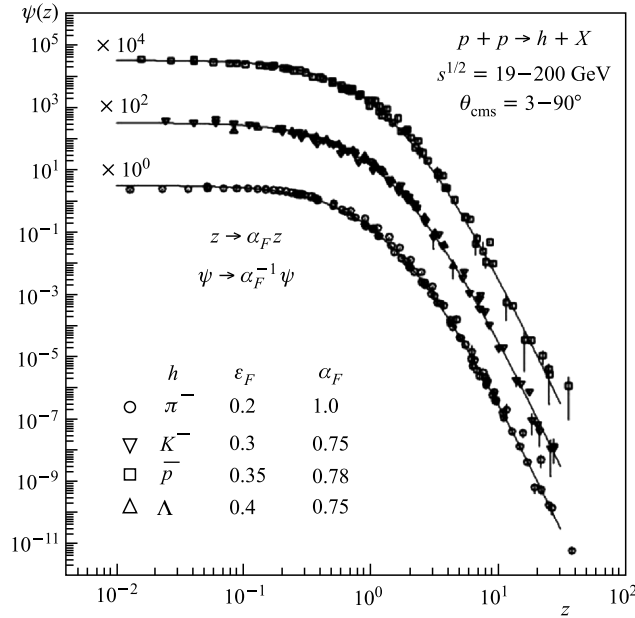


Fig. 5. Inclusive spectra of the hadrons produced in proton–proton collisions in the  $z$ -presentation. The symbols denote the experimental data obtained in the experiments performed at CERN, FNAL, and BNL [6, 7]

and processes of fragmentation into real registered particles. The fractal dimension  $\varepsilon_F$  of the fragmentation process varies for different types of hadrons. The scale transformation  $z \rightarrow \alpha_F z, \Psi \rightarrow \alpha_F^{-1} \Psi$  results in the compatibility of the corresponding scaling curves in the plane  $\{z, \Psi\}$ . The normalization condition (6) is conserved by the transformation.

As is seen from Fig. 5, the scaling function  $\Psi(z)$  exhibits two kinds of behavior: one in the low- $z$  and the other one in the high- $z$  region. The low- $z$  region corresponds to saturation of the scaling function with the typical flattening-out. The behavior of  $\Psi(z)$  at low  $z$  depends only on parameter  $c$ . This parameter is determined from the multiplicity dependence of the spectra. The region of low  $z$  (the transverse momentum  $< 100$  MeV) and of high multiplicity density is preferable (even in proton–proton interactions) to study the collective effects and observe the phase transition in the hadron matter. The low- $z$  region is best suited for studying the collective phenomena in the systems of hadrons and their constituents. The region of high  $z$  (a high transverse momentum) is characterized by the power behavior of  $\Psi(z) \sim z^{-\beta}$  with the constant value of slope  $\beta$ . At high  $z$ , the observed power behavior of the scaling function points to self-similarity in constituent interactions at small scales. The asymptotic behavior of  $\Psi(z)$  imposes restrictions on the behavior of the cross sections at high  $p_T$ . The restrictions can be used to perform the global QCD fit and construct quark and gluon distribution functions in the regions where the experimental data are missing.

The parameters  $\delta, \varepsilon_F$ , and  $c$ , introduced to construct variable  $z$ , are determined from analyses of many different sets of experimental data [5–10]. They are shown to be constant and independent of the kinematic quantities — the collision energy, angle and transverse momenta of the inclusive particle, and multiplicity density. A possible change of the parameters can be used as a signature of new phenomena in the kinematic regions not yet explored experimentally. This is primarily true for the low ( $z < 0.01$ ) and high ( $z > 10$ ) regions of the variable  $z$ . In the intermediate region ( $0.01 < z < 10$ ), the shape of  $\Psi(z)$  is well determined from the data in the kinematic range which is now accessible for experiments at the current accelerators. Note that extension of the  $z$  range does not require obligatory increase in the collision energy. It is possible when rare events are specially selected for super low  $z$  (e.g.,  $p_T < 100$  MeV/ $c$  at  $s_{NN}^{1/2} = 200$  GeV) or super high  $z$  (e.g.,  $p_T > 4$  GeV/ $c$  at  $s_{NN}^{1/2} = 9.2$  GeV or  $p_T > 30$  GeV/ $c$  at  $s_{NN}^{1/2} = 200$  GeV). A more stringent restriction on the scaling behavior of  $\Psi(z)$  at high  $z$  would bear witness to self-similarity at scales smaller than  $10^{-4}$  fm related with the notion of fractal space-time. In the new LHC energy range, a check of the regularities found earlier over the whole  $z$  range is of interest: either the indicated properties of  $z$ -scaling will be confirmed or a deviation from the universal behavior of  $\Psi(z)$  will be observed.

#### 4. SCALING IN AA COLLISIONS

The phase transitions and other collective effects must show up in a larger space volume in the collisions of heavy nuclei than in proton–proton interactions. It is expected that they influence the production mechanism of particles, i.e., interaction of nuclear constituents, as well as the fragmentation process in the final state. The modification of the latter is due to the specific properties (high density and temperature in a larger volume) of the medium produced in the nuclear collisions.

The inclusive spectra of the charged hadrons produced in Au + Au collisions at different centralities and energies  $s_{NN}^{1/2} = 200$  and 9.2 GeV are shown in Figs. 6, *a* and *b*. The data [35, 36] were obtained by the STAR collaboration at the RHIC. A consistent description of the data in  $z$ -presentation has been obtained by the condition that the fractal dimension of the nucleus  $\delta_A$  is expressed in terms of the nucleon fractal dimension  $\delta$  and the atomic number of nucleus  $\delta_A = A\delta$  [5]. It has been found that the specific heat (parameter  $c$ ) is independent

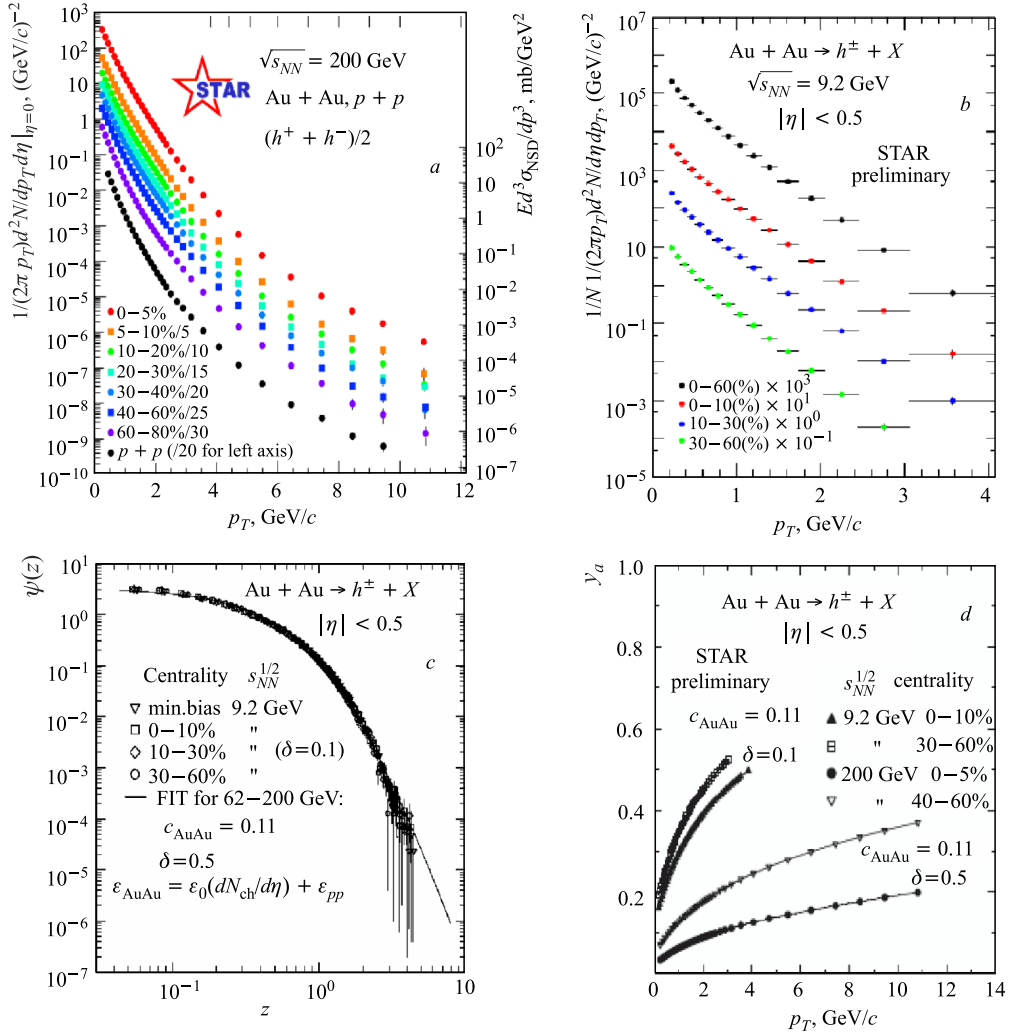


Fig. 6. Inclusive spectra of the charged hadrons produced in Au+Au collisions in the central rapidity range, at different centralities and energies  $s_{NN}^{1/2} = 200$  GeV (*a*) and 9.2 GeV (*b*). Symbols are the data obtained by the STAR collaboration [35, 36]. *c*) The scaled presentation of the preliminary data at  $s_{NN}^{1/2} = 9.2$  GeV. The solid line is a fitted curve for the data at  $s_{NN}^{1/2} = 62.4, 130,$  and 200 GeV [35, 39, 40]. *d*) Dependence of fraction  $y_a$  on the transverse momentum, centrality, and collision energy [36]

of the centrality of the collision and decreases with increase of the atomic number of the nucleus. A strong suppression of the function  $\Psi(z)$  with the increasing centrality in nuclear collisions has been found for the centrality-independent value of  $\varepsilon_{AA}$ . The suppression is enhanced with the increasing transverse momentum  $p_T$ . The universal shape of  $\Psi(z)$  for  $A + A$  collisions can be restored if the dependence of the fractal dimension  $\varepsilon_{AA}$  of the fragmentation process on the event centrality (multiplicity density) is assumed. It was taken in the following form:

$$\varepsilon_{AA} = \varepsilon_0 \left( \frac{dN_{\text{ch}}}{d\eta} \right) + \varepsilon_{pp}. \quad (7)$$

The value of  $\varepsilon_{pp}$  is the same as for proton–proton collisions. The coefficient  $\varepsilon_0$  depends on the collision energy. Similar behavior has been observed for the interaction of nuclei (Cu, Au, and Pb) at other energies  $s_{NN}^{1/2} = 17.3, 62.4, \text{ and } 130 \text{ GeV}$  [37, 38]. Illustration of the unique shape of the scaling function  $\Psi(z)$  obtained under the above conditions is shown in Fig. 6, *c*. In the low- $z$  region, saturation of  $\Psi(z)$  similar to that revealed in proton–proton collisions [6, 7] has been observed. The saturation region ( $z < 0.1$ ) is of interest to study the events with large multiplicities. In the region of small  $z$  (low  $p_T$ ), the effect of the Coulomb nuclear field modifies the spectra of charged particles. Therefore, more precise information on the behavior of the function  $\Psi(z)$  in this region can be obtained from the analysis of spectra of neutral particles (for example, neutral strange  $K_S^0$  mesons and  $\Lambda^0$  hyperons).

The shape of the scaling function at low  $z$  (low  $p_T$ ) is governed by the parameter  $c$  which is interpreted as the specific heat of the produced medium. The value of  $c$  was found to be constant in Au + Au collisions at  $s_{NN}^{1/2} = 9.2, 62.4, 130, \text{ and } 200 \text{ GeV}$ . Discontinuity of this parameter would be assumed as a signature of the phase transition or vicinity of the critical point.

Figure 6, *d* shows the  $p_T$ -dependence of the fraction  $y_a$  on centrality in Au + Au collisions at  $s_{NN}^{1/2} = 9.2$  and 200 GeV. The behavior of  $y_a$  demonstrates monotonic growth with  $p_T$ . It means that the energy loss  $\Delta E \sim 1 - y_a$  associated with the production of a high- $p_T$  hadron is smaller than for the hadron with a lower transverse momentum. The decrease of  $y_a$  with centrality corresponds to a larger energy loss in central collisions as compared with peripheral interactions. The energy loss grows with the collision energy. For central Au + Au collisions at  $p_T \approx 3 \text{ GeV}/c$ , it is estimated to be about 55% at  $s_{NN}^{1/2} = 9.2 \text{ GeV}$  and 90% at  $s_{NN}^{1/2} = 200 \text{ GeV}$ , respectively.

## 5. SEARCH FOR PHASE TRANSITION IN HEAVY-ION COLLISIONS

In this section we discuss possibilities of using  $z$ -scaling approach to search for critical phenomena in relativistic collisions of heavy nuclei. The endeavor for a unique description of the spectra of the hadrons produced in  $A + A$  interactions by universal scaling function  $\Psi(z)$  gives strong restriction on the parameters of  $z$ -scaling. A sharp change (or discontinuity) of the fractal dimensions  $\delta_A, \varepsilon_{AA}$  or heat capacity  $c$  is offered as a signature of new effects, in particular of the phase transition. Such effects can be, however, smeared by a large energy loss especially in the central collisions of heavy nuclei. The growth of  $\varepsilon_{AA}$  with the collision centrality (multiplicity) corresponds to the increased energy losses of the secondary particles in the produced medium at their fragmentation. This contributes to difficulties in

the localization of the region where the phase transition or the critical point could be expected. The problem can be partially evaded in the cumulative region where the energy losses are small.

This holds for the hard cumulative processes corresponding to the region  $x_1 A_1, x_2 A_2 > 1$  with production of the high transverse momentum particles. Such processes were not investigated earlier. The transition into the cumulative region at fixed centrality is considered as an essential condition of searching for the phase transition and localization of the critical point.

A microscopic scenario of the interaction between hadrons and nuclei at the level of the interacting constituents, developed within the framework of  $z$ -scaling, predicts the dependence of the energy losses on the collision energy and centrality, transverse momentum and type of the inclusive particle, and order of cumulativity.

Figure 7 illustrates the microscopic scenario for the pion production in Au + Au collisions at the energies  $s_{NN}^{1/2} = 9.2$  and 200 GeV, where the  $p_T$ -dependences of the following quantities are depicted: the fraction  $x_1 A_1$  of the nucleon momentum carried by the interacting constituent (a); the momentum fraction  $y_a$  of the scattered constituent carried away by the inclusive particle (b); the mass  $M_X$  of the recoil system in the constituent interaction which balances the production of the inclusive particle (c). Study of the dependence of the cumulative number  $x_1 A_1$  on centrality is of special interest. As seen from Fig. 7, a, the cumulative region  $x_1 A_1, x_2 A_2 > 1$  is attainable only at lower energies. The relationship between the cumulative number and the centrality at the energy  $s_{NN}^{1/2} = 9.2$  GeV is weaker than at  $s_{NN}^{1/2} = 200$  GeV over the entire indicated range of the transverse momentum  $p_T$ . This is related with the energy loss  $\Delta E \sim 1 - y_a$  by the production of the inclusive particle. The decrease of the energy loss with the increasing  $p_T$  is very significant especially at lower energies and high transverse momenta (Fig. 7, b) which corresponds to the cumulative region  $x_1 A_1 > 1$  (Fig. 6, a). Here the reduction of the collision energy results in effective reduction in energy losses of the secondary particles upon their fragmentation into the observed hadrons. However, very small collision energy is undesirable because it tends to decrease the inclusive channels of the reaction.

As seen from Fig. 7, a, the kinematical region, which corresponds to the cumulative numbers 1–2, covers the momentum range  $p_T = 4$ –8 GeV/c for the pions produced in Au + Au collisions at  $s_{NN}^{1/2} = 9.2$  GeV close to an angle of  $90^\circ$  in the  $N$ – $N$  center-of-mass system. Changes and correlations among the parameters  $\delta_A, \varepsilon_{AA}$ , and  $c$  are expected in this region. Here the fractal dimension  $\delta_A$  can be sensitive to particle-like fluctuations (fluctons) of the colliding nuclei. The fragmentation properties of the particles produced in the collisions of fluctons could influence the value of fragmentation dimension  $\varepsilon_{AA}$ . Information on the properties of the produced medium in the collisions of the cumulated nuclei could change the known value of the specific heat  $c$ . The sensitivity of the fractal dimensions and specific heat to flucton interactions can be enhanced with the increased order of cumulativity ( $x_1 A_1, x_2 A_2$ ). Determining the dependence of the fractal dimensions on the order of cumulativity, we can study the structure of the fluctons themselves. We expect that the fractal dimension  $\delta_A$  will grow with the order of cumulativity. It should be greater for the flucton substructure (the local cumulation of the nuclear matter in the nucleus) than for the ordinary nucleus. The found relation  $\delta_A = A\delta$  for nuclei may be violated and in the cumulative region it can be as follows:  $\delta_A = A^d\delta$ ,  $d > 1$ .

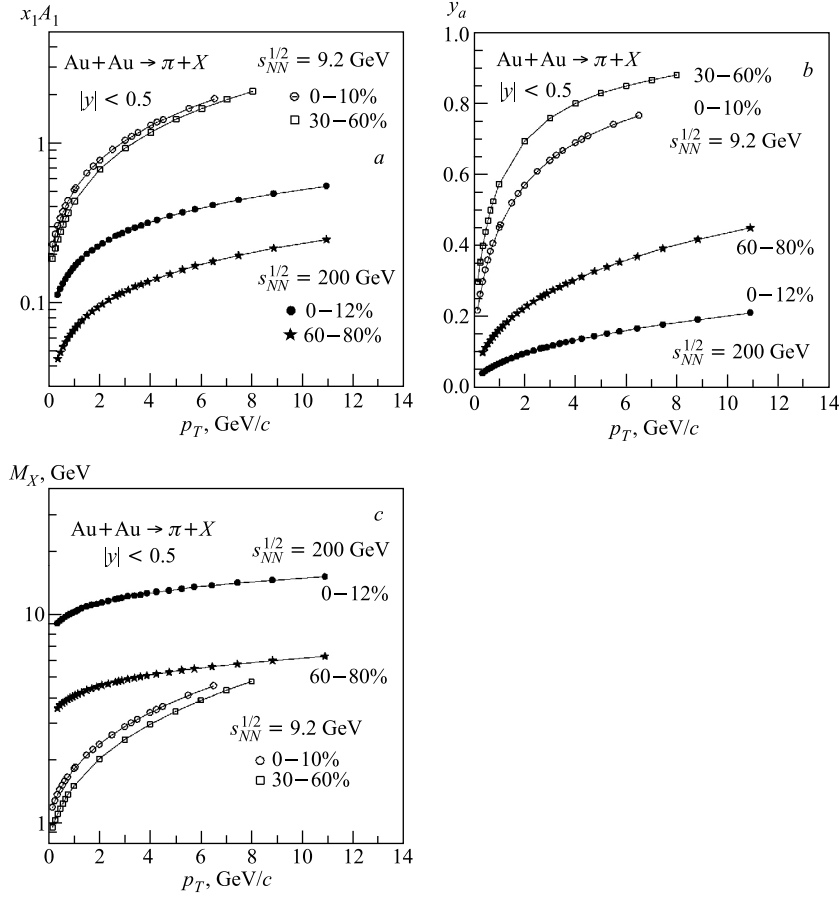


Fig. 7. Dependence of the fractions  $x_1 A_1$  (a),  $y_a$  (b), and recoil mass  $M_X$  (c) on the transverse momentum of the inclusive particle produced in Au + Au collisions at different energies  $s_{NN}^{1/2} = 9.2$  and 200 GeV, centrality, and  $|y| < 0.5$  [41]

The most stringent condition in the cumulative region is multiplicity which can be used to select events to control the properties of the medium in which the flucton interactions take place. It is expected that the transition into the cumulative region with high multiplicity events may involve additional selection of events with higher density of the nuclear matter. The smaller energy loss with additional compression of the nuclear matter can allow us to find more accurate localization of the critical point and detection of the phase transition.

The transverse momentum dependence of the mass  $M_X$  of the nonregistered recoil system is shown in Fig. 7, c. The values of  $M_X$  grow steeply with the transverse momentum at the energy  $s_{NN}^{1/2} = 9.2$  GeV when compared with their increase at  $s_{NN}^{1/2} = 200$  GeV. Similar to the cumulative number in Fig. 6, a, the sensitivity of the recoil mass to centrality is small at lower energy. The relatively large values of  $M_X$  at the energy  $s_{NN}^{1/2} = 9.2$  GeV for high transverse momenta reflect peculiarities of the cumulative region and evoke connections with the notion of a cumulative jet.

## CONCLUSION

Search for clear signatures of the phase transition of the nuclear matter and location of the critical point in heavy-ion collisions at SPS and RHIC has been discussed. The experimental data on the inclusive spectra of hadrons measured in Au + Au collisions at RHIC over a wide range of the collision energy  $s_{NN}^{1/2} = 9\text{--}200$  GeV were analyzed in the framework of  $z$ -scaling. The requirement of the universal description of the hadron spectra in nuclear collisions at different energies and centralities gives restrictions on the values of the parameters of  $z$ -scaling and their dependences on the multiplicity density. The parameters  $\delta_A$ ,  $\varepsilon_{AA}$ , and  $c$  are interpreted as the fractal dimension of the nuclear structure, fractal dimension of the fragmentation process, and the heat capacity of the produced medium, respectively. The scaling regularity reflects the self-similarity property of the structure of the colliding objects, interaction mechanism of their constituents, and process of fragmentation. The microscopic scenario of the constituent interactions in the framework of  $z$ -scaling approach was discussed. The dependences of the constituent energy loss, order of cumulativity, and the mass of the recoil system on the momentum of the produced hadron, energy and centrality of the collision have been studied. It is motivated by the fact that the hadron production in the cumulative region ( $x_1 A_1, x_2 A_2 > 1$ ) is a preferable regime to search for signatures of the phase transition and the critical point in heavy-ion collisions. In our opinion, the most optimal energy region for these experimental studies corresponds to the energies  $s_{NN}^{1/2} = 10\text{--}40$  GeV covered by the Beam Energy Scan Programs carried out at the accelerators SPS (CERN) and RHIC (BNL).

**Acknowledgements.** The investigations have been supported by the IRP AVOZ10480505, by the Ministry of Education, Youth and Sports of the Czech Republic's grants LA08002, LA08015, and by the special program of the Ministry of Science and Education of the Russian Federation, grant RNP.2.1.1.2512.

## REFERENCES

1. Marcinek A. (for the NA61 Collab.) // Rencontres de Moriond «QCD and High Energy Interactions», La Thuile, France, March 13–20, 2010;  
Gazdzicki M. (for the NA61/SHINE Collab.) // J. Phys. G. 2009. V. 36. P. 064039.
2. Caines H. (for the STAR Collab.) // Proc. of the Rencontres de Moriond 2009, QCD session; nucl-ex/0906.0305v1;  
Abelev B. I. et al. (STAR Collab.). <http://drupal.star.bnl.gov/STAR/starnotes/public/sn0493>;  
Abelev B. I. et al. (STAR Collab.) // Phys. Rev. C. 2010. V. 81. P. 024911.
3. Polyakov A. M. // Zh. Eksp. Teor. Fiz. 1970. V. 59. P. 542; 1971. V. 60. P. 1572.
4. Koba Z., Nielsen H. B., Olesen P. // Nucl. Phys. B. 1972. V. 40. P. 317.
5. Tokarev M. V. et al. // Intern. J. Mod. Phys. A. 2001. V. 16. P. 1281.
6. Zborovský I., Tokarev M. V. // Phys. Rev. D. 2007. V. 75. P. 094008.
7. Zborovský I., Tokarev M. V. // Intern. J. Mod. Phys. A. 2009. V. 24. P. 1417.
8. Tokarev M. V., Zborovský I., Dedovich T. G. // Proc. of Very High Multiplicity Physics Workshops / Ed. by A. Sissakian, J. Manjavidze. Singapore, 2008. P. 97.
9. Zborovský I., Tokarev M. V. // Phys. At. Nucl. 2009. V. 72. P. 552.
10. Tokarev M. V. // Ibid. P. 541.

11. Stanley H. E. Introduction to Phase Transitions and Critical Phenomena. London: Oxford Univ. Press, 1971.
12. Widom B. // J. Chem. Phys. 1965. V. 43. P. 3829; 3898.
13. Hankey A., Stanley H. E. // Phys. Rev. B. 1972. V. 6. P. 3515.
14. Stanley H. E. // Rev. Mod. Phys. 1999. V. 71. P. S358.
15. Kadanoff L. P. // Physics. 1966. V. 2. P. 263.
16. Kadanoff L. P. et al. // Rev. Mod. Phys. 1967. V. 39. P. 395.
17. Kadanoff L. P. // Proc. of the 1970 Varenna Summer School on Critical Phenomena / Ed. by M. S. Green. N. Y., 1971.
18. Fisher M. E. // Rep. Prog. Phys. 1967. V. 30. P. 615.
19. Fisher M. E. // Rev. Mod. Phys. 1974. V. 46. P. 597.
20. Fisher M. E. // Rev. Mod. Phys. 1998. V. 70. P. 653.
21. Domb C. The Critical Point: A Historical Introduction to the Modern Theory of Critical Phenomena. London: Taylor & Francis, 1996.
22. Cardy J. Scaling and Renormalization in Statistical Physics. Cambridge Univ. Press, 1996.
23. Patashinskii A., Pokrovskii V. // Fluctuation Theory of Phase Transitions. Intern. Series in Natural Philosophy. Pergamon Press, 1979. V. 98. P. 321.
24. Kadanoff L. P. // Statistical Physics. River Edge, NJ, 2000. P. 483.
25. Rushbrooke G. S. // J. Chem. Phys. 1963. V. 39. P. 842.
26. Griffiths R. B. // Phys. Rev. Lett. 1965. V. 14. P. 623.
27. Fisher M. E. // J. Math. Phys. 1963. V. 4. P. 124; Physica. 1960. V. 26. P. 816; 1028.
28. Josephson B. D. // Proc. Phys. Soc. 1967. V. 92. P. 269.
29. Coopersmith M. H. // Phys. Rev. 1968. V. 167. P. 478; Phys. Rev. Lett. 1968. V. 20. P. 432.
30. Guggenheim E. A. // J. Chem. Phys. 1945. V. 13. P. 253.
31. Lubbeck S. // Intern. J. Mod. Phys. B. 2004. V. 18. P. 3977.
32. Kutateladze S. S. Analysis of Self-similarity and Physical Models. Novosibirsk: Nauka, 1986.
33. Van Dyke M. An Album of Fluid Motion. Stanford, California: The Parabolic Press, 1982.
34. Strukov B. A. // Soros Educat. J. 1996. V. 12. P. 95.
35. Adams J. et al. (STAR Collab.) // Phys. Rev. Lett. 2003. V. 91. P. 172302.
36. Tokarev M. V. (for the STAR Collab.). nucl-ex/1004.5582.
37. Tokarev M. V., Zborovský I. // Part. Nucl., Lett. 2010. V. 7, No. 3. P. 171.
38. Tokarev M. V., Zborovský I. // Nonlin. Phen. Comp. Syst. 2009. V. 12. P. 459.
39. Adler C. et al. (STAR Collab.) // Phys. Rev. Lett. 2002. V. 89. P. 202301.
40. Gagliardi C. A. (for the STAR Collab.) // Eur. Phys. J. C. 2005. V. 43. P. 263.
41. Tokarev M. V., Zborovský I. // Part. Nucl., Lett. 2010. V. 7, No. 3. P. 160.